

## DISCRETE SATURATION OF THE ELECTRON PARAMAGNETIC RESONANCE

SPECTRUM OF  $U^{3+}$  IN  $CaF_2$ 

P. I. BEKAURI, B. G. BERULAVA, T. I. SANADZE, O. G. KHAKHANASHVILI, and G. R. KHUTSISHVILI

Tbilisi State University

Submitted February 17, 1970

Zh. Eksp. Teor. Fiz. 59, 368-376 (August 1970)

The electron paramagnetic resonance spectrum of  $U^{3+}$  in  $CaF_2$  in an environment of tetragonal symmetry is studied by the discrete saturation (DS) technique. The observed complex fluorine hyperfine structure can be explained by the interaction of the paramagnetic center with the nine nearest nuclei of  $F^-$  ions. A study of the DS spectra in the three principal orientations of the crystal with respect to the external magnetic field  $H$  yields complete information on the hyperfine interaction tensor for the nuclei closest to the paramagnetic center. The hyperfine interaction parameter for nuclei of the second coordination sphere is estimated.

THE present work is the first attempt to use the phenomenon of discrete saturation (DS)<sup>[1,2]</sup> of the EPR line to investigate the hyperfine interaction (HFI) of a paramagnetic center with the nuclei surrounding it in the case of a monocrystalline substance. As the object of investigation, we chose  $CaF_2$  with a  $U^{3+}$  impurity in an environment of tetragonal symmetry. The EPR spectrum in this substance was studied earlier by Bleaney, Llewellyn, and Jones,<sup>[3]</sup> who established a model for the immediate environment of the paramagnetic center and observed complicated fluorine hyperfine structure (HFS) for certain orientations of the crystal with respect to the external magnetic field  $H$ . In<sup>[4]</sup>, an attempt was made to explain the fluorine HFS in a simple-spectrum model, i.e., without taking account of reorientation of the nuclear spins during the electron transition. Later, however, we observed DS in the EPR spectrum of this substance,<sup>[1]</sup> and this indicates the important contribution of transitions with reorientation of the nuclear spins for the UHF band used ( $\lambda = 3.2$  cm and  $\lambda = 1.7$  cm). This latter fact has also found confirmation in the recent work of Chau, Chapellier, and Goldman,<sup>[5]</sup> in which interesting modulation effects at high frequencies were explained.

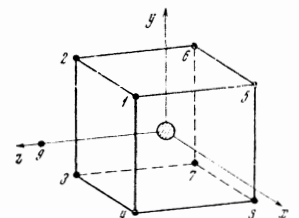
As will be shown below, the DS method has turned out to be very effective for the explanation of the observed fluorine HFS. Furthermore, this method has enabled us to obtain complete information on the HFI tensor for the nuclei nearest to the paramagnetic center.

Monocrystals of  $CaF_2$  are a simple cubic lattice of  $F^-$  ions, with  $Ca^{2+}$  ions at the centers of alternate cubes formed by the  $F^-$  ions. A tetragonal center of the trivalent impurity  $U^{3+}$  is formed by replacement of  $Ca^{2+}$ . To compensate the charge, there is an extra  $F^-$  ion at the center of the neighboring empty cube of  $F^-$  ions. The paramagnetic center is thus situated in an environment of nine  $F^-$  ions (cf. Fig. 1). Eight of these are positioned at the vertices of the cube, and the ninth along one of the  $[100]$  directions. This extra  $F^-$  ion lowers the symmetry of the environment of the paramagnetic center from cubic to tetragonal. The EPR spectrum is explained by the three equivalent ions with significantly anisotropic g-factors.

To obtain the DS spectra we used the technique described in<sup>[1]</sup>. Powerful UHF pulses ( $\approx 0.1$  watt) of approximate duration  $10 \mu\text{sec}$  were applied to a small portion of the EPR line with continuous sinusoidal modulation (at the frequency of the supply system) of the magnetic field, encompassing the whole line. The time intervals between the UHF pulses were longer than the spin-lattice relaxation time  $T_1$ , so that there was time for the line to recover its shape completely. For the samples investigated, a liquid-helium temperatures, this time was approximately 1 sec. A simple synchronization scheme enabled us to apply the UHF pulse repeatedly to any chosen portion of the EPR line. The DS spectrum was observed on the screen of an oscilloscope with a driven sweep triggered by the UHF pulse. The true shape of the absorption curve (with strong attenuation of the saturating UHF pulse) or a curve with a DS spectrum (when the UHF pulses were applied without attenuation) could be obtained alternately on the oscilloscope.

Oscillograms of the DS spectra and the initial shape of the absorption curve in different orientations of the crystal with respect to the external field  $H$  are shown in Fig. 2. The oscillogram 1 corresponds to  $H$  directed along the z-axis (see Fig. 1), and oscillogram 2 to  $H$  directed along the x- or y-axis. In these principal orientations, (1 -  $H \parallel z$  or 2 -  $H \perp z$ ), the ninth nucleus does not contribute to the DS spectrum, since these directions are also principal axes for the HFI tensor  $A_{ijk}$ . From symmetry arguments it is easy to see that the tensor  $A_{ijk}$ <sup>[9]</sup> has diagonal form in the xyz coordinate system. Because of this, the DS spectra in the above orientations are due to the eight nuclei immediately

FIG. 1. Model of the immediate environment of  $U^{3+}$ .



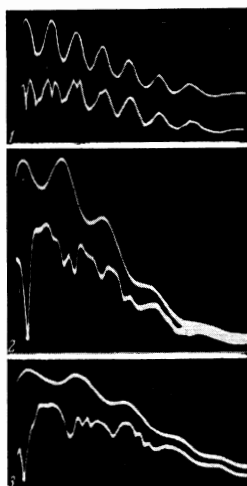


FIG. 2. Oscillograms of the DS spectra (lower) and of the true shape of the absorption curve (upper) for three orientations of the magnetic field: 1)  $-H \parallel [001]$ , 2)  $-H \parallel [010]$ , 3)  $-H \parallel [110]$ .

surrounding the paramagnetic center. In the orientations corresponding to oscillograms 1 and 2, these nuclei are, to a good approximation, equivalent.

The scheme of the levels for eight equivalent nuclei is given in Fig. 3. As was indicated in [2], the saturation of a given pair of levels, e.g., of the pair indicated by an arrow in Fig. 3, leads to the appearance of two subsystems of DS lines, with parameters  $\epsilon_+$  and  $\epsilon_-$ . These quantities give the spacings in the upper and lower levels corresponding to the electron spin projections  $m = \pm 1/2$ . For convenience we have shown, by continuous lines, only those transitions which are observed in the oscillogram (Fig. 2). It is essential to note that, on saturation of a given part of the EPR line, a DS pattern can be observed only to the right or only to the left of the saturated part (apart from the case when the spectral diffusion time is longer than the period of modulation of the magnetic field, when it is possible, by a repeated scanning, to see the whole DS spectrum).

If we can ignore the weak lines of the DS spectrum, the nature of which will be discussed below, two subsystems of DS lines, corresponding to the parameters  $\epsilon_+$  and  $\epsilon_-$ , are easily detected in orientation 2. In orientation 1, only one parameter is observed, whence we can conclude that  $\epsilon_+ = \epsilon_-$ . These parameters have been measured by means of the narrow HFS reference lines of nitrogen in silicon carbide or by using the observed structure in the EPR line.

The expressions for  $\epsilon_+$  and  $\epsilon_-$ <sup>1)</sup>

$$\epsilon_{\pm} = [(\hbar\gamma H \mp \frac{1}{2}A_{\parallel})^2 + \frac{1}{4}A_{\perp}^2]^{1/2} \quad (1)$$

(where  $A_{\parallel}$  and  $A_{\perp}$  denote the components of the vector  $\mathbf{A}_n$  in the direction along  $\mathbf{H} = H\mathbf{n}$  and in the plane perpendicular to  $\mathbf{H}$ ), together with the formulae (8) and (12) of [2], enable us to determine all the parameters necessary for the calculation of the HFS spectrum. The expected spectrum was constructed from formula (14) of

<sup>1)</sup>In expression (1) we have changed the sign of  $\gamma$  from what it was in [2]; this is physically justified and necessary for a correct analysis of the signs of the components of the HFI tensor. It is also essential to note that formula (1) is valid only for an isotropic g-factor or for magnetic field directions corresponding to the principal values of the g-factor.

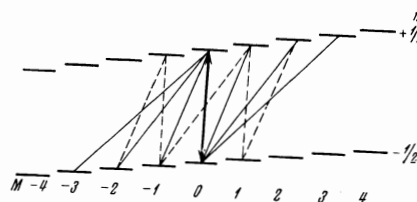


FIG. 3. Scheme of the levels for eight equivalent nuclei with spin  $1/2$ ;  $m$  and  $M$  are the projections of the electron spin and the total nuclear spin. (Because of the fact that the directions of the effective magnetic fields do not coincide even for equivalent nuclei,  $M$  has no physical meaning; it is, however, a convenient parameter for grouping the levels.)

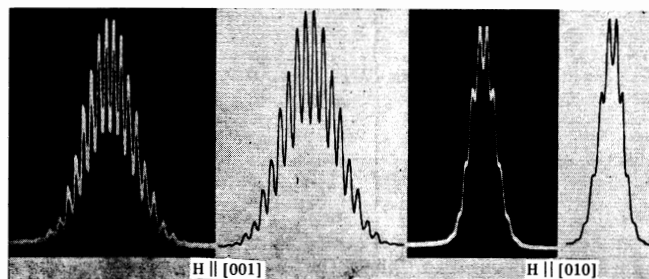


FIG. 4. The observed fluorine HFS and the calculated absorption lineshapes for the orientations  $H \parallel [001]$  and  $H \parallel [010]$ .

[2], which in the present case takes the form

$$[p(x^s + x^{-s}) + q(x^r + x^{-r})]^s (x^{\delta} + x^{-\delta}). \quad (2)$$

Here  $s = \frac{1}{2}(\epsilon_+ - \epsilon_-)$  and  $r = \frac{1}{2}(\epsilon_+ + \epsilon_-)$ ;  $q$  and  $p$  are the relative probabilities of electron transitions with and without reorientation of a nuclear spin;  $\delta$  is the level-splitting due to the ninth nucleus. On changing the UHF band, the parameters  $s$  and  $r$  change owing to the change of  $\hbar\gamma H$ , while  $\delta$  remains constant. This parameter was determined by comparing the HFS spectra at wavelengths 3.2 and 1.7 cm.

The following values were obtained for the parameters necessary for the construction of the HFS spectra in orientations 1 and 2.

Orientation 1 ( $H \parallel z$ ;  $g_{\parallel} = 3.501$ ):

$$\begin{aligned} \epsilon_+ = \epsilon_- = 4.05 \pm 0.08 \text{ Oe}; \quad s = 0, \quad r = 4.05; \\ p = 0.15, \quad q = 0.85, \quad \delta = 11.2 \pm 0.4 \text{ Oe}; \end{aligned}$$

Orientation 2 ( $H \perp z$ ;  $g_{\perp} = 1.866$ ):

$$\begin{aligned} \epsilon_+ = 7.3 \pm 0.15 \text{ Oe}, \quad \epsilon_- = 5.7 \pm 0.15 \text{ Oe}; \quad s = 0.8, \quad r = 6.5; \\ p = 0.73, \quad q = 0.27, \quad \delta = 7.9 \pm 0.8 \text{ Oe}. \end{aligned}$$

In orientation 2 there is uncertainty in the subscripts of the quantities  $\epsilon$ , but, as is clear from formula (2), this does not affect the result of the calculation of the HFS spectrum.

The expression (2) gives the intensities  $a_i$  and positions  $H_i$  for all transitions. The enveloping EPR line was constructed, using a computer, from the formula  $\sum a_i \exp[-(H - H_i)^2/2b^2]$ , with Gaussian components whose second moment  $b$  was determined from the HFS spectrum and was equal to 1.1 Oe. This parameter could also be estimated from the DS spectrum, as will be discussed below.

The oscillograms of the HFS spectra in orientations 1 and 2 and the calculated spectra are shown in Fig. 4. The calculated spectra for the UHF band  $\lambda = 3.2$  cm

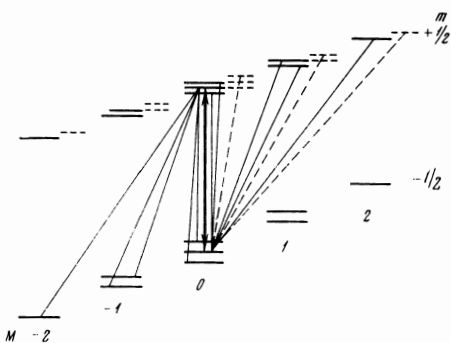


FIG. 5. Level-scheme for two pairs of inequivalent nuclei. The saturated transition is indicated by an arrow.

(just as for  $\lambda = 1.7$  cm) coincide completely, in all details, with those observed experimentally.

We shall now consider the weak lines in the DS spectra, which appear between the main troughs in the spectra 1 and 2 of Fig. 2. In the case of orientation 1 ( $\mathbf{H} \parallel z$ ) it was possible to assume that these gaps arise because of the non-equivalence of nuclei 1-4 relative to nuclei 5-8 (see Fig. 1); this can be taken into account in a general form by introducing splittings  $\epsilon_+ - \epsilon'_+$  and  $\epsilon_- - \epsilon'_-$  in the upper and lower levels in a manner analogous to that shown in simpler form in Fig. 5 for two pairs of non-equivalent nuclei. Here  $\epsilon_{\pm}$  and  $\epsilon'_{\pm}$  are, respectively, the level splitting parameters for nuclei of the two groups. We examined several complex variants of level-schemes, but none of them was found to correspond to the observed DS spectrum. Moreover, all these complicated level schemes gave parameters  $\epsilon_{\pm}$  and  $\epsilon'_{\pm}$  such that using them made the agreement of the calculated and observed HFS line shapes worse.

On the other hand, these weak lines in the DS spectrum can be simply explained by taking the  $F^-$  nuclei of the second coordination sphere into account. For these nuclei, the expected values of the HFI tensor components  $A_{ijk}$  must be approximately an order of amplitude smaller than for the  $F^-$  nuclei immediately surrounding the  $U^{3+}$ , i.e., about 1 Oe, which gives  $\epsilon_{\pm} \approx \hbar\gamma H = 1.58$  Oe. This value is very close to the observed 1.6-Oe spacings between the weak and the main DS lines. Thus, the main lines in the DS spectra in orientation 1 are caused by the nuclei immediately surrounding the paramagnetic center, whereas the weak lines positioned in the intervals between them are due to the  $F^-$  nuclei of the second coordination sphere. From a given DS spectrum (by observing the intensities of the weak lines) one can estimate the magnitude of the HFI tensor components:  $A_{ijk} \approx 1$  Oe. This order of magnitude of the tensor components determines the width of the separate components of the spectrum of the nuclei of the immediate environment, and is in good agreement with the second moment used in the calculations of the spectrum shown in Fig. 4.

In the crystal orientation corresponding to oscillogram 2 in Fig. 2 ( $\mathbf{H} \parallel x$  or  $\mathbf{H} \parallel y$ ), the weak lines in the DS spectrum are not explained by the level-scheme shown in Fig. 3. And, unlike in orientation 1, they cannot be caused by  $F^-$  nuclei of the second coordination sphere, since in the given case,  $\hbar\gamma H = 5.57$  Oe and the corresponding transitions will have negligibly small probabilities ( $\hbar\gamma H \gg A$ ).

On saturation of a definite part of the EPR line, two processes can lead to the formation of a spectrum of troughs:

- 1) DS processes, which are transitions independent of concentration;
- 2) discrete cross-relaxation processes within the EPR line or "discrete spin-diffusion processes," first observed by Feher and Gere<sup>[6]</sup> in silicon alloyed with arsenic. These processes depend on the concentration of paramagnetic centers.

Experimentally it is easy to distinguish these two processes. If the DS spectra can be observed immediately following the application of a saturating pulse and only spread out over a period of time, a certain amount of time is needed for the troughs to develop appreciable depth so that the second process can be observed.

The weak lines in the DS spectrum in orientation 2 (see Fig. 2) are caused by discrete spectral diffusion processes. This could be easily verified by increasing the magnetic field modulation index. On increasing the sweep rate of the magnetic field by a factor of about 10, the weak lines in the DS spectra disappeared, while the main lines remained unchanged.

The formation of these troughs is illustrated in Fig. 3 by the dotted lines. In fact, after saturation by a UHF pulse of the pair of levels indicated by an arrow in Fig. 3, owing to discrete spin diffusion processes, the adjacent levels reach a state of partial saturation. In Fig. 3 they are indicated by vertical dotted lines. The transitions associated with these levels will also be in a state of partial saturation. Some of these are shown by sloping dotted lines. This picture is in complete agreement with the position of the weak lines in orientation 2 (see Fig. 2).

As was shown above, by measuring  $\epsilon_+$  and  $\epsilon_-$  from the DS spectra, one can easily explain the observed HFS in the respective orientations. The known values of  $\epsilon_+$  and  $\epsilon_-$  determine the parameters  $A_{\parallel}$  and  $A_{\perp}$  from relation (1). From these data one can measure all the tensor components  $A_{ijk}$ , if the measurements are carried out in several orientations of the crystal with respect to the external field  $\mathbf{H}$ .

By simple transformations we can obtain relations connecting the tensor components  $A_{ijk}$  with the parameters  $A_{\parallel}$  and  $A_{\perp}$ :

$$A_{\parallel} = \alpha_i \alpha_k A_{ik}, \quad A_{\parallel}^2 + A_{\perp}^2 = \alpha_i \alpha_k A_{pi} A_{pk}; \quad (3)$$

Here  $\alpha_i$  are the direction cosines of the magnetic field  $\mathbf{H}$  with respect to the  $x$ ,  $y$ , and  $z$  axes ( $i, k, p = x, y, z$ ).

As was shown in the paper of Baker, Davies, and Hurrell,<sup>[7]</sup> the HFI tensor is, in the general case, asymmetric. For the nucleus 1 shown in Fig. 1, the HFI tensor, in the coordinate frame  $x'y'z'$  with axes directed along  $[1\bar{1}0]$ ,  $[11\bar{2}]$  and  $[111]$  and in the  $xyz$  coordinate frame respectively, should have the form:<sup>2)</sup>

$$\hat{a} = \begin{pmatrix} a_1 & 0 & 0 \\ 0 & a_2 & a_5 \\ 0 & a_4 & a_3 \end{pmatrix}, \quad \hat{A} = \begin{pmatrix} A_1 & A_2 & A_5 \\ A_2 & A_1 & A_5 \\ A_4 & A_4 & A_3 \end{pmatrix}. \quad (4)$$

The zero terms in the  $x'y'z'$  coordinate frame occur because of the presence of the reflection plane

<sup>2)</sup>Following [2], we write the HFI in the form  $\hat{A}\hat{S}$ , in contrast to [7], where it was written as  $\hat{S}\hat{A}$ . Therefore, our matrices are transposed with respect to the matrices  $\hat{A}$  of [7].

( $\bar{1}\bar{1}0$ ). For the nuclei 2, 3, and 4, the HFI tensor in the xyz coordinate frame has the same form, except that the signs of the off-diagonal elements change. The nuclei 5–8 are, generally speaking, not equivalent to the nuclei 1–4. We denote the corresponding matrices of the HFI tensor by  $\hat{a}'$  and  $\hat{A}'$ .

It is essential to note that, in fact, the model pictured in Fig. 1 undergoes distortion. In reality, the cube is deformed by the impurity  $U^{3+}$  ion and the interstitial  $F^-$  ion;<sup>[7]</sup> what is important is that the ( $\bar{1}\bar{1}0$ ) reflection plane remains unchanged, as also does the system of axes xyz. Experimentally, the true values of the components of the tensor  $\hat{A}$  are determined.

To determine the five parameters of the HFI tensor it is necessary to make measurements in three independent orientations. Three magnetic field orientations were chosen:  $\mathbf{H} \parallel [001]$  (orientation 1),  $\mathbf{H} \parallel [100]$  (orientation 2), and  $\mathbf{H} \parallel [110]$  (orientation 3). In these orientations the relations (3) are greatly simplified.

Orientation [001]:

$$A_{\parallel} = A_3, \quad A_{\perp} = \sqrt{2}A_5; \quad (5a)$$

Orientation [100]:

$$A_{\parallel} = A_1, \quad A_{\perp} = \sqrt{A_2^2 + A_4^2}; \quad (5b)$$

Orientation [110]:

$$\begin{aligned} A_{\parallel} &= A_1 + A_2, & A_{\perp} &= \sqrt{2}A_4 - \text{nuclei 1, 3 and 5, 7;} \\ A_{\parallel} &= A_1 - A_2, & A_{\perp} &= 0 - \text{nuclei 2, 4 and 6, 8.} \end{aligned} \quad (5c)$$

The DS spectra corresponding to these orientations are given in Fig. 2. In orientations 1 and 2, these spectra were discussed above.

In orientation 3, the inequivalence of the nuclei of the group 1–4 on the one hand and those of the group 5–8 on the other is resolved. In this orientation only two pairs of equivalent nuclei, namely nuclei 1 and 3 and nuclei 5 and 7, contribute to the DS spectrum. For the remaining nuclei of the immediate environment we have  $A_{\perp} = 0$  and this automatically excludes them from the DS spectrum, since the direction of the effective field at the nuclei coincides with the direction of the external field.<sup>[2]</sup>

The level-scheme for the two pairs of non-equivalent nuclei, corresponding to orientation 3, is given in Fig. 5. In this scheme, the possible levels are arranged for simplicity in the following order:

$$-e_+ - e_+ \left| \begin{array}{c} -e_+ \left| \begin{array}{c} e_+ - e_+' \\ 0 \\ -e_+' \end{array} \right| \begin{array}{c} e_+' \\ e_+' \\ e_+' \end{array} \end{array} \right| \begin{array}{c} e_+' \\ e_+' \\ e_+' \end{array}$$

and analogously for  $e_-$ . The transition saturated by the UHF pulse is indicated by an arrow. The transitions observed in oscillogram 3 of Fig. 2 are shown by continuous lines.

In order to verify the correctness of this scheme of levels, we performed a calculation of the intensities of the lines in the expected DS spectrum. For this it was necessary to expand the expression

$$[p(x^+ + x^-) + q(x^+ + x^-)]^2 [p'(x^+ + x^-) + q'(x^+ + x^-)]^2 \quad (6)$$

and identify the transitions corresponding to the lines of the DS spectrum. The parameters occurring in formula (6) can be determined experimentally and are ex-

pressed in terms of  $e_+$ ,  $e_-$ ,  $e_+'$ , and  $e_-'$ . The exact calculation of the intensities is complicated, for two reasons. On saturation of a given part of the EPR line, as shown by an arrow in Fig. 5, other levels, displaced by intervals  $\pm(e_+ - e_+' )$  and  $\pm(e_- - e_-' )$ , will also be saturated. Their presence is due to the inhomogeneous broadening of the EPR line by the nuclei not contributing to the DS spectrum, i.e., by the  $F^-$  nuclei 2, 4, 6, and 8 (in the [110] orientation), and also by nuclei of the second coordination sphere. These nuclei do not take part in the level-scheme in Fig. 5, but cause a continuous shift in it. To avoid overloading Fig. 5, we show, by a dotted line, only one displaced level-scheme which is saturated along with the central transition. Together with this, the presence of discrete spectral diffusion also changes the intensities of the transitions slightly. In spite of all this, an approximate calculation gives a DS spectrum which is in good agreement with that observed experimentally.

In orientation 3, the parameters  $e_+ + e_+'$  and  $|e_+ - e_+'|$  and also  $e_- + e_-'$  and  $|e_- - e_-'|$  can be determined directly. The uncertainty in the sign of the differences of the  $e$  leads to two alternative sets of values for  $e_+$ ,  $e_-$ , and  $e_+'$ ,  $e_-'$ . In addition there is uncertainty in the subscript  $\pm$  of the parameters  $e$  (which depend on the sign of  $A_{\parallel}$ ).

In a specific case, these uncertainties can be circumvented. In fact the parameters  $A_{\parallel}$  and  $A_{\perp}$  determined in orientations 1 and 2 are close to each other. It follows from this fact that the cubic approximation for the HFI tensor is a good one. In the approximation of cubic symmetry,  $A_1 = A_3$  and  $A_2 = A_4 = A_5$ . In our case, the parameters  $A_1$  and  $A_3$  are small compared with the off-diagonal terms; in particular,  $A_3 = 0$  (since, in orientation 1,  $e_+ = e_-$ ). This indicates that the dipole-dipole interaction is dominant for the HFI tensor, and this enables us to determine the sign of  $A_2$  ( $A_2 > 0$ )<sup>[7]</sup> (the diagonals of a cube are at the magic angle to the x, y, and z axes). From this, we obtain the sign of the parameter  $A_{\parallel}$  in orientation 3:  $A_{\parallel} = A_1 + A_2 > 0$ , which removes the uncertainty in the subscripts of the parameters  $e$  in orientations 3 and 2.

In orientation 2, the non-equivalence of the nuclei of the two groups (nuclei 1–4 and 5–8) is not resolved (if this non-equivalence were resolved, there would be no difficulty in obtaining the components of the HFI tensor from the conditions (5)). However, from this orientation we have two conditions, determined from the width of the troughs and the measured average values  $\bar{\epsilon}_+$  and  $\bar{\epsilon}_-$ :

$$|e_+ - e_+'| < |e_- - e_-'| \leq 0.5 \text{ Oe}, \quad (7)$$

$$\bar{\epsilon}_+ = \frac{1}{2}(e_+ + e_+'), \quad \bar{\epsilon}_- = \frac{1}{2}(e_- + e_-' ). \quad (8)$$

The latter inequality in condition (7) follows from the fact that in orientation 3 the parameter  $|e_+ - e_+'| = 0.6 \text{ Oe}$  is now easily resolved in the DS spectrum.

In Eqs. (8) the right-hand sides can be expressed in terms of  $A_1$  and  $A_1'$  using Eqs. (1) and (5). Two equations are obtained, in terms of square-roots, with two unknowns. A graphical method was found to be the most convenient for solving this system of equations.

The problem of finding the parameters  $A_1$  and  $A_1'$  for the alternative sets of parameters  $e$  determined from orientation 3 has, in our case, a unique solution

$A_{ik}$	Nuclei 1-4		Nuclei 5-8		Nucleus 9	
	Oe	MHz	Oe	MHz	Oe	MHz
$A_1$	$-1.9 \pm 0.2$	$-4.9 \pm 0.5$	$-1.8 \pm 0.2$	$-4.7 \pm 0.5$	$-7.9 \pm 0.8$	$-20 \pm 2$
$A_2$	$3.2 \pm 0.2$	$8.3 \pm 0.5$	$5.2 \pm 0.2$	$13.6 \pm 0.5$	0	0
$A_3$	$0 \pm 0.1$	$0 \pm 0.5$	$0 \pm 0.1$	$0 \pm 0.5$	$11.2 \pm 0.4$	$55 \pm 2$
$A_4$	$4.7 \pm 0.2$	$12.3 \pm 0.5$	$5.2 \pm 0.2$	$13.6 \pm 0.5$	0	0
$A_5$	$5.3 \pm 0.1$	$26.0 \pm 0.5$	$5.3 \pm 0.1$	$26.0 \pm 0.5$	0	0

satisfying condition (7). The values obtained for the components of the HFI tensors are given in the table.

As has been shown above, interpreting the DS spectra in the presence of equivalent nuclei presents no difficulty. The accuracy of the information obtained in the HFI tensor exceeds the requirements of present-day quantum-chemical calculations, but is significantly inferior to that of the analogous measurements obtained by the electron-nuclear double resonance method. In addition, in arbitrary orientations of the magnetic field in the presence of a large number of nuclei in the environment of the magnetic center, the number of transitions in the DS spectrum increases sharply because of the inequivalence of the nuclei, whereas in electron-nuclear double resonance the number of lines does not exceed  $2l$ , where  $l$  is the number of nuclei. Nevertheless, in certain cases, as has been shown in the example of  $U^{3+}$  in  $CaF_2$ , to study the HFI of a paramagnetic center with the surrounding nuclei the DS method is convenient to use because of the simplicity of both the experimental technique and the interpretation of the spectra obtained. In some cases, this method can be applied in conjunction with electron-nuclear double resonance to determine the necessary radio-frequency band and to give a preliminary interpretation of the spectra before the values of the HFI tensor components are obtained more accurately.

The authors express their thanks to Prof. P. P. Feofilov for providing the monocrystals.

Note added in proof (July 15, 1970). Further investigation of the reason for the appearance of the weak lines in the DS spectrum in orientation 2 has shown that they are caused, basically, by saturation of forbidden transitions for F nuclei of the second coordination sphere. The disappearance of these troughs on rapid scanning of the line by the magnetic field in the experiments described above was due to a change in the conditions for saturation of the forbidden transitions.

<sup>1</sup>P. I. Bekauri, B. G. Berulava, T. I. Sanadze, and O. G. Khakanashvili, Zh. Eksp. Teor. Fiz. **52**, 447 (1967) [Sov. Phys.-JETP **25**, 292 (1967)].

<sup>2</sup>T. I. Sanadze and G. R. Khutsishvili, Zh. Eksp. Teor. Fiz. **56**, 454 (1969) [Sov. Phys.-JETP **29**, 248 (1969)].

<sup>3</sup>B. Bleaney, P. M. Llewellyn, and D. A. Jones, Proc. Phys. Soc. **69B**, 858 (1956).

<sup>4</sup>B. G. Berulava, T. I. Sanadze, and O. G. Khakanashvili, Zh. Eksp. Teor. Fiz. **48**, 437 (1965) [Sov. Phys. Phys.-JETP **21**, 288 (1965)].

<sup>5</sup>V. H. Chau, M. Chapellier, and M. Goldman, J. de Phys. **30**, 427 (1969).

<sup>6</sup>G. Feher and E. A. Gere, Phys. Rev. **114**, 1245 (1959).

<sup>7</sup>J. M. Baker, E. R. Davies, and J. P. Hurrell, Proc. Roy. Soc. **A308**, 403 (1968).

Translated by P. J. Shepherd